Journal of Materials Chemistry B

Accepted Manuscript

ROYAL SOCIETY OF CHEMISTRY

www.rsc.org/materialsB

Synthesis of Diblock/Statistical Cationic Glycopolymers with Pendant Galactose and Lysine Moieties: Gene Delivery Application and Intracellular Behaviors

Jingjing Sun[1], Ruilong Sheng[1, 2], Ting Luo[1], Zhao Wang[1], Hui Li[1] and Amin Cao*[1]*

1. *Key Laboratory of Synthetic and Self-assembly Chemistry for Organic Functional Molecules, Shanghai Institute of Organic Chemistry, CAS. Lingling Road 345, Shanghai, 200032, China.*
2. *Department of Chemistry, Université de Montréal, Succursale Centre-ville, Montreal, Quebec, H3C3J7, Canada.*

**Author for correspondence*

Phone: +86-21-54925535

Email: rlsheng@mail.sioc.ac.cn; acao@mail.sioc.ac.cn;

Abstract

New series of cationic block copolymers PHML-*b*-PMAGal and statistical copolymers P (HML-*st*-MAGal) with pendant natural galactose and (*l*-)-lysine moieties were prepared via RAFT (reversible addition-fragmentation chain-transfer) polymerization. The block/statistical copolymers showed high plasmid DNA binding affinity (N/P<2) and the as-formed polyplexes were spherical nanoparticles with the average size of 100~300 nm and surface zeta potentials of +30.2~+46.3 mV. The cytotoxicity and gene transfection efficacy of the PHML-*b*-PMAGal and P (HML-*st*-MAGal) vectors strongly depended on the polymer architectures (block/statistical) and galactose contents. Notably, the statistical copolymer P(HML_{40}-*st*-$MAGal_4$) with 4.8% galactose content showed the highest gene transfection efficiency among the synthesized cationic polymers, 6.8-folds higher than that of the "gold standard" bPEI-25K in the presence of 10% FBS (Fetal bovine serum) in various cell lines. Intracellular uptake mechanism (with 10% FBS) study demonstrated that the P(HML_{40}-*st*-$MAGal_4$)/pDNA polyplexes mainly entered into H1299 cells through caveolae-mediated endocytosis and microtubule-dependent endocytosis pathway. Moreover, the fluorescent imaging study showed the P(HML_{40}-*st*-$MAGal_4$)/pDNA polyplexes possessed obvious "lysosomal escaping" effect that led to efficient pDNA release, which might interpret the fact of the significant increase of the related gene transfection efficiency. Moreover, it could be anticipated that the P(HML_{40}-*st*-$MAGal_4$) cationic glycopolymer might be employed as low toxic, high efficient and serum-compatible gene carriers for practical application.

Key Words: cationic diblock glycopolymer, cationic statistical glycopolymer, gene delivery, serum-compatible, endocytosis pathway

1. Introduction

In the past few decades, cationic polymeric non-viral gene vectors have been developed as a new technique for gene therapy, and it is well known that successful gene therapy largely depends on the choice of suitable building blocks in construction of the cationic polymeric gene vectors[1-4]. Although many cationic polymeric vectors were developed to mediate efficient intracellular gene transfection, some defects such as high cytotoxicity[5], immunogenicity[6] and low serum- compatibility[7, 8] severely restricted their clinical application in gene therapy. To solve these issues, a general approach in previous works is to conjugate/modify cationic polymers with polyethylene glycol (PEG), which could be employed to shield cationic surface charge, decrease cytotoxicity and improve serum-compatibility of cationic polymer vector/gene complexes [5, 9]. However, it should be noted that the "stealth" effect of PEG could decrease cell adhesion and intracellular uptake, further resulting in lower transfection efficiency of the polyplexes[10]. Moreover, the PEG-modified polymeric vectors might induce immune-response as antigens and would be erased by macrophage systems after injection[11].

Recently, several biocompatible building blocks such as zwitterionic molecules[12, 13] and carbohydrates [14] have been developed as alternative substitutes to PEG moieties in gene/drug delivery systems. Among them, carbohydrates are highly biocompatible natural products with good hydrophilicity and biodegradable manners. It had been disclosed that cationic glycopolymer vectors constructed by carbohydrates and cationic units exhibited low cytotoxicity and serum-resist stability, which resembled that of the PEG-conjugated polycations due to the positive charge shielding effect. But unlike PEG, the carbohydrates units in glycopolymers have the advantage of enhancing pDNA binding affinity through hydrogen bond interactions, which may further facilitate high gene transfection efficiency [15-18]. Besides, the multi-hydroxyl groups on carbohydrate units offered them the possibility for further functional derivation/modification [19, 20]. e. g. Azzam et al [21] synthesized some polyethylenimine and spermine modified dextran and branched-starch cationic polymers, found the gene transfection capability largely relied on the polysaccharide structures, and dextran-derived cationic polymers showed the highest transfection capability. Davis et al [22] reported that the length of cationic blocks played essential roles in the cytotoxicity and gene transfection of cyclodextrin-based cationic gene vectors. Gu et al [23] prepared (*l*)-lysine-modified chitosan polymers, which exhibited high *in-vitro* gene transfection capability and low cytotoxicity. However, due to the

complicated and uncontrollable structures of these natural polysaccharide glycopolymers, it is difficult to elucidate their concise structure-activity relationships. Thus, developing new cationic glycopolymers with defined and controllable molecular structures as efficient gene vectors/carriers is of high demand.

With the development of controlled free radical polymerization, a lot of functional glycopolymers with well-defined structures and controllable molecular-weight could be facilely prepared [24, 25], which made it possible for further investigating the correlation between polymer structure and gene transfection related properties. e. g. Narain et al synthesized a series of well-defined block and random glycopolymers as gene vectors and found the latter showed higher gene transfection efficiency than the former one [26-29]. Reineke et al prepared some cationic glycopolymers as gene vectors and disclosed that introducing of sugar-containing blocks could increase the stability of pDNA-loaded complexes by preventing their aggregation in culture medium [14, 30-33]. However, to our knowledge, many cationic building blocks used for constructing glycopolymeric gene vectors were non- biodegradable or low-biocompatible. Alternatively, cationic amino acids (such as (*l*)-lysine and (*l*)-arginine) serve as essential biocompatible natural cationic building blocks for constructing new cationic gene vectors with low cytotoxicity and high pDNA binding affinity [34, 35]. Moreover, some cationic glycopolymers constructed by amino acids and carbohydrates could act as high efficient synthetic mimics of natural virus-based gene vectors [36, 37]. However, up to now, design and synthesis of well-defined cationic amino acid-based glycopolymer gene carriers with low cytotoxicity, high gene transfection efficiency and preferred serum-compatibility is still a challenge. Besides, the structure-activity relationships and intracellular features (especially precise mechanisms of intracellular uptake and trafficking) of the amino acid-based glycopolymer gene carrier systems are still far from clear and need to be deeply investigated.

To develop new amino acid-based cationic glycopolymers with well-defined structures and elucidate the structure-dependent gene transfection properties, in this work, a series of diblock (PHML-*b*-PMAGal) and statistical (P(HML-*st*-MAGal)) cationic glycopolymers with pendant galactose and (*l*)-lysine moieties were synthesized by RAFT polymerization. The cytotoxicity, *in vitro* luciferase (Luc) gene transfection efficacy and the impact of serum on the gene transfection efficiency were evaluated in various cell lines. Finally, the cellular uptake/endocytosis pathway and intracellular localization of the glycopolymers/pDNA payloads were investigated and discussed.

2. Experimental Procedures

2.1. Materials

4-cyano-4-(dodecylsulfanylthiocarbonyl)sulfanyl pentatonic acid were synthesized according to the literature [38]. HEMA-Boc-Lys monomer was synthesized according to our previous work [39]. Synthesis of the glycomonomer 6-O-methacryloyl-1, 2, 3, 4-di-O-isopropylidene-galactopyranose (MAIGal) was depicted in S1 (supporting information). Tetrahydrofuran (THF) was dehydrated by refluxing with sodium and purified by distillation before use. 2, 2-Azobis(isobutyronitrile) (AIBN) was obtained from Shanghai Sinopharm Chemical Reagent Co., Ltd. (China) and was purified by recrystallization in ethanol. Branched polyethylenimine (bPEI-25K, M*w*=25,000, Cat#408727) and Thiazoyl blue tetrazolium bromide (Cat#M2128) were purchased from by Sigma & Aldrich. Lysotracker (Cat#L7526) was purchased from Invitrogen (USA). Label IT tracker™ intracellular nucleic acid localization kit was purchased from Mirus Bio Corporation (Cat#MIR7010, USA). Luciferase assay and bicinchoninic acid (BCA) protein quantitation kits were supplied by Promega (Cat#E1500, USA) and Biomiga (Cat#PW0104, USA), respectively. 0.1 M phosphate buffer solution (PBS 1×), MEM, RPMI-1640 medium and Dulbecco's modified eagle media (DMEM) were purchased from Hangzhou Genom Co. Ltd. Fetal bovine serum (FBS) was supplied by GIBCO (Cat#10099-141, USA) and ExCell Bio (Cat#FSP500,China). DAPI was received from Roche (Cat#70217321, Switzerland). The pCMV-Luc plasmid and COS-7 cell lines were generously gifted by Prof. Yuhong Xu of school of pharmacy of Shanghai Jiaotong University (Shanghai, China). H1299, SK-HEP-1, CHO, HeLa and MCF-7 cell lines were generously gifted by Dr. Bo Wan in Fudan University (Shanghai, China). All other chemicals and solvents were of analytical grade and were used as received.

2.2. Preparation of the glycopolymers

2.2.1. Synthesis of PHMLBoc

To a dried Schlenk tube equipped with magnetic stirring bar, HEMA-Boc-Lys (2.88 g，6.2 mmol), 4-cyanopentanoic acid dithiobenzoate (16 mg, 0.062 mmol), AIBN (2.5 mg, 0.0155 mmol) and 5 mL dried tetrahydrofuran was added. The mixture was deoxygenated by freeze-pump-thawing for three times, and then immersed into an oil bath thermostated at 70°C for 5 h under N_2 protection. Afterward, the reaction was quenched by immersing the Schlenk tube into liquid nitrogen and the

mixture was precipitated in hexane, filtrated and dried in vacuum to give pink powder as the PHMLBoc product.

^{1}H NMR (300 MHz, $CDCl_3$, δ in ppm): 5.64, 5.15 (N*H*COO, 2H, br), 4.48-4.06 (OCH_2CH_2O, COC*H*(R) NH, 5H, brm), 3.10 (NHCH_2COOR, 2H, m), 2.06-1.49 (CH_2, CH_2-CCH_3, 8H, brm), 1.44 (C (CH_3)$_3$, 9H, s), 1.24-0.76 (C-CCH_3, 3H, brm)

FTIR (in cm^{-1}): 3380, 2977, 2933, 2867, 1714, 1520, 1456, 1392, 1366, 1250, 1170, 1050, 866, 737, 668

2.2.2. Synthesis of PHMLBoc-*b*-PMAIGal polymers

PHMLBoc (0.93 g，0.05 mmol), MAIGal (0.13 g, 0.4 mmol), AIBN (2.5 mg, 0.0155 mmol) and 2 mL dried tetrahydrofuran was added into a dried Schlenk tube, which was deoxygenated by freeze-pump-thawing for three times, and then immersed into an oil bath thermostated at 90°C for 24 h. Afterward, the mixture was precipitated in hexane, filtrated and dried in vacuum to give the PHMLBoc-*b*-PMAIGal as pink powder.

^{1}H NMR (300 MHz, $CDCl_3$, δ in ppm): 5.68, 5.17 (br, N*H*COO), 5.51(s, Galactopyranose (Gal)-H at 1 position), 4.63 (m, Gal-H at 3 position), 4.62-3.87 (brm, OCH_2CH_2O, COC*H*(R)NH, Gal-H at 2, 4, 5 position), 3.10 (m, NHCH_2COOR), 2.06-1.49 (brm, CH_2, CH_2-CCH_3), 1.44 (s, C(CH_3)$_3$), 1.24-0.76 (brm, C-CCH_3)

FTIR (in cm^{-1}): 3378, 2976, 2932, 1715, 1521, 1456, 1392, 1366, 1250, 1169, 1052, 864, 781

2.2.3. Synthesis of P(HMLBoc-*st*-MAIGal) polymers

MAIGal (42.6 mg，0.13 mmol), HEMA-Boc-Lys (0.6 g，1.3 mmol), AIBN (1.2 mg, 0.0076 mmol), 4-cyanopentanoic acid dithiobenzoate (8 mg, 0.031 mmol) 4 mL toluene was added into a dried Schlenk tube, which was deoxygenated by freeze-pump-thawing for three times, and then immersed into an oil bath thermostated at 90°C for 24 h. Afterward, the mixture was precipitated in hexane, filtrated and dried in vacuum to give the P(HMLBoc-*st*-MAIGal) as pink powder.

^{1}H NMR (300 MHz, $CDCl_3$, δ in ppm): 5.68, 5.17 (br, N*H*COO), 5.51 [s, Galactopyranose (Gal)-H at 1 position], 4.63 (m, Gal-H at 3 position), 4.62-3.87 (brm, OCH_2CH_2O, COC*H*(R)NH, Gal-H at 2, 4, 5 position), 3.10 (m, NHCH_2COOR), 2.06-1.49 (brm, CH_2, CH_2-CCH_3), 1.44 (s, C(CH_3)$_3$), 1.24-0.76 (brm, C-CCH_3)

FTIR (in cm^{-1}): 3378, 2976, 2932, 1715, 1521, 1456, 1392, 1366, 1250, 1169, 1052, 864, 781

2.2.4. Preparation of PHML, PHML-*b*-PMAGal and P (HML-*st*-MAGal) cationic polymers

The as-prepared PHMLBoc, PHMLBoc-*b*-PMAIGal and P(HMLBoc-*st*-MAIGal) polymer precursors were deprotected at room temperature in mixed trifluoroacetic acid (TFA) and tetrahydrofuran (THF) (2/1, v/v) for 24 h, and then precipitated in cold diethyl ether, filtrated and dried in vacuum, the final cationic polymer products were obtained as white solids.

PHML:

^{1}H NMR (D_2O, δ in ppm): 4.48-3.90 (COOCH_2CH_2O, COCH(R)NH, 5H, brm), 2.83 (CH_2N, 2H, t), 2.02-1.20 (CH_2-CCH_3, CH_2, 8H, brm), 0.94-0.58 (C-CCH_3, 3H, d).

PHML-*b*-PMAGal:

^{1}H NMR (300 MHz, DMSO-d_6, δ in ppm): 8.72, 8.08 (s, N$H_3^+CF_3COO^-$), 4.62-3.83 (brm, OCH_2CH_2O), 3.17 (s, Galactose hydroxyl groups), 2.78 (s, -NHCH_2COOR), 2.07-1.21 (brm, CH_2, CH_2-CCH_3), 1.04-0.52 (brm, C-CCH_3)

FTIR (in cm^{-1}): 3431, 1679, 1539, 1433, 1203, 1136, 966, 839, 801, 723

P (HML-*st*-MAGal):

^{1}H NMR (300 MHz, DMSO-d_6, δ in ppm): 8.72, 8.08 (s, N$H_3^+CF_3COO^-$), 4.62-3.83 (brm, OCH_2CH_2O), 3.17 (s, Galactose hydroxyl groups), 2.78 (s, -NHCH_2COOR), 2.07-1.21 (brm, CH_2, CH_2-CCH_3), 1.04-0.52 (brm, C-CCH_3)

FTIR (in cm^{-1}): 3431, 1679, 1539, 1433, 1203, 1136, 966, 839, 801, 723

2.3. Instrumental Characterization of the synthesized cationic polymers.

NMR spectrum: ^{1}H NMR spectrum were conducted on a Varian-300 FT-NMR spectrometer at 300.0 MHz for proton nuclei, and ^{13}C NMR was implemented on a Bruker Avance-400 NMR spectrometer, operating at 100.0 MHz for ^{13}C nuclei, tetramethylsilane (TMS) was used as internal chemical shift reference in all NMR measurements.

FT-IR spectra: FT-IR spectra were recorded on a Bio-Rad FTS-185 spectrometer at room temperature in the wavelength ranging from 4000 to 500 cm^{-1} with 4 cm^{-1} spectral resolution (64 times scanning).

Gel permeation chromatography (GPC): Average molecular weights (M_n and M_w) and polydispersity index (M_w/M_n) of the glycopolymer precursors were measured at 35°C on a PerkinElmer 200 GPC equipped with a refractive index detector (RI). Tetrahydrofuran was utilized as the eluent at a flowing rate of 1.0 mL/min, and a series of commercial polystyrene standards (*Polymer laboratories, UK*) were applied to calibrate the GPC elution traces.

2.4. Agarose gel electrophoresis

pDNA binding affinity of the PHML, PHML-*b*-PMAGal and P(HML-*st*-MAGal) cationic polymers were determined by agarose gel electrophoresis. Each cationic polymer/pDNA polyplexes were prepared by mixing cationic polymers with 1 μg pDNA at various N/P charge ratios in deionized water. After 30 min incubation at 37°C, the mixed solution was loaded onto agarose gel (1.2% w/v) containing ethidium bromide (0.1 mg/ml in gel) in TAE buffer solution, commercially available DNA markers and naked pDNA were used as controls. The electrophoresis was run at 100 V for 40 min. Finally, the pDNA retardation was observed and recorded using a UV transilluminator (UVP, USA).

2.5. Average particle size and Zeta potential measurements by DLSs

Each cationic polymer/pDNA polyplexes were prepared by mixing cationic polymers with 1 μg pDNA (1 mL solution) at various N/P charge ratios in deionized water. Average particle sizes and Zeta potential values of the PHML/pDNA, PHML-*b*-PMAGal/pDNA and P(HML-*st*-MAGal)/pDNA polyplexes were measured by dynamic scattering instrument (Malvern Zetasizer Nano ZS90, UK, λ=633 nm, scattering angle of 90°) at 25°C.

2.6. Transmission electronic microscopy (TEM)

The morphology of the $PHML_{40}$/pDNA, $PHML_{40}$-*b*-$MAGal_3$/pDNA and P(HML_{40}-*st*-$MAGal_4$)/ pDNA polyplexes were measured by TEM (JEOL-1230, *JEOL Co. Ltd, Japan*) with an acceleration voltage of 80 KV. For each sample preparation, the polyplex solution (1.0 mg/mL) was dropped onto a 300-mesh carbon-coated copper grid, excess solution was absorbed and removed with filter paper, and the grid was then air-dried at room temperature.

2.7. MTT cytotoxicity assay

In vitro cytotoxicity of the PHML, PHML-*b*-PMAGal and P(HML-*st*-MAGal) cationic polymers was evaluated by MTT assay in H1299 cells. First, H1299 cells were seeded into 96-well microplates at a density of 5.0×10^3 cells/well in 100 μL of RPMI-1640 medium containing 10% FBS. After 24 h incubation, the culture medium was replaced with fresh RPMI-1640 medium (100 μL, with 10% FBS), and predetermined amounts of cationic polymers were added and further incubated for another

24 h. Then 20 μL of MTT solution (5 mg/mL) was added into each well and incubated for additional 2 h at 37°C. After that, the medium was discarded and 100 μL/well DMSO was added with mildly shaken for 10 min to dissolve the formed MTT formazan. The absorbance of all samples was measured with six replicates (n=6) by using microplate reader (BioTek, ELx800, USA) at λ=490 nm (λ=630 nm as the reference wavelength). Relative cell viability (%) was calculated according to the equation: Relative cell viability (%) = $(OD490_{sample}-OD630_{sample})/(OD490_{control}-OD630_{control}) \times 100\%$

2.8. *In vitro* luciferase gene transfection assay

For *in vitro* luciferase gene transfection assay of the PHML, PHML-*b*-PMAGal and P(HML-*st*-MAGal) cationic polymers, first, H1299 cells were seeded in 24-well plates (4×10^5 cells/well) with 500 μL of RPMI-1640 medium containing 10% FBS. After incubation for 24 h, the medium were replaced with 500 μL fresh RPMI-1640 medium (10% FBS) containing the polyplex (1 μg pDNA/well) at various charge ratios and further incubated for 24 h at 37 °C, the commercially available bPEI-25k (N/P=10) was used as the control. The luciferase assay was performed according to the protocols and relative light units (RLUs) were measured with the Promega GloMax®-Multi Single Tube Multimode Reader (E6070, USA), protein quantification was determined by BCA assay kit (*Applygen Technologies Inc, China*) according to the protocol, and relative light unit per milligram of Luciferase protein (RLU/mg) was calculated to evaluate the cell transfection efficacy of the cationic polymers (n=3).

For *in vitro* luciferase gene transfection assay of the optimized P(HML_{40}-*st*-$MAGal_4$)/pDNA polyplexes (N/P=40) in the presence of serum, the SK-HEP-1, MCF-7, CHO, HeLa and COS-7 cells were separately seeded into 24-well plates (1×10^5 cells/well) with 500 μL of MEM (SK-HEP-1 cells), DMEM (MCF-7, CHO and HeLa cells) or RPMI-1640 (COS-7 cells) medium (all the medium are containing 10% FBS). After incubation for 24 h, the medium were replaced with fresh medium (+10% FBS) with the P(HML_{40}-*st*-$MAGal_4$)/pDNA polyplex (1 μg pDNA/well, N/P=40) and further incubated for 24 h at 37 °C. The luciferase gene expression assay was performed as the protocols showed above with commercially available bPEI-25k (N/P=10) as the control.

2.9. Endocytosis mechanism/pathway of the P(HML_{40}-*st*-$MAGal_4$)/pDNA polyplexes

Endocytosis mechanism/pathway of the P(HML_{40}-*st*-$MAGal_4$)/pDNA polyplexes was measured by

flow cytometry with various endocytosis-specific inhibitors. First, H1299 cells were seeded into 24-well microplates (4×10^5 cells/well) and further cultivated overnight in RPMI 1640 medium containing 10% FBS. Then, the medium in microplates were replaced with fresh RPMI 1640 medium (+ 10% FBS). Endocytosis inhibitors including amiloride (2.25 μg/mL, macropinocytosis inhibitor), chloropromazine (3.0 μg/mL, clathrin-mediated endocytosis inhibitor), nocodazole (2.0 μg/mL, microtubule inhibitor) and methyl-β-cyclodextrin (M-β-CD, 2.5 mM, caveolae-mediated endocytosis inhibitor) were respectively added into each well and incubated for 1 h. Subsequently, the cells were replaced with fresh RPMI 1640 medium (with 10% FBS) and dealt with the as-prepared P (HML_{40}-*st*-$MAGal_4$)/pDNA polyplex (1 μg pDNA/well, N/P=40). After incubation for 24 h, the luciferase gene expression assay was performed as the protocols showed above.

2.10. Intracellular trafficking of the P(HML_{40}-*st*-$MAGal_4$)/Cy3-pDNA polyplexes

H1299 cells were seeded into 6-well microplates (4×10^5 cells/well in 1 mL of RPMI 1640 medium with 10% FBS) and incubated under 37 °C and 5% CO_2 for 24 h. The P(HML_{40}-*st*-$MAGal_4$)/ Cy3-pDNA polyplexes were prepared by mixing Cy3-labeled pDNA with P(HML_{40}-*st*-$MAGal_4$) polymer (N/P=40) and incubated at 37 °C for 30 min [35]. The as-prepared P(HML_{40}-*st*-$MAGal_4$)/ Cy3-pDNA polyplexes was added into the well and incubated for predetermined time (2 h and 6 h). Then the H1299 cells were washed with 1×PBS for three times to eliminate fluorescence background. The cells were fixed with 4% paraformaldehyde in 0.12 M phosphate buffer (pH=7.4) for 10 min and washed with 1×PBS for three times. Lysotracker (final working concentration 100 ng/mL) was added to stain the endosome/lysosome and incubated for 15 min before fluorescence imaging. Finally, the intracellular localization of the P(HML_{40}-*st*-$MAGal_4$)/Cy3-pDNA polyplexes were visualized and recorded on a Nikon Ti-S invert fluorescence microscopy.

3. Results and discussion

3.1. Preparation and characterization of the cationic polymers

In order to prepare new cationic glycopolymers with the merit of well-defined, functionalized and controllable structures, and to further study the effect of the functional building blocks and glycopolymers structures (block *vs* statistical) on the related physico-chemical and biological properties, a homopolymer PHML with pendent (*l*)-lysine, and series of block glycopolymers PHML-*b*-PMAGal and statistical glycopolymers P(HML-*st*-MAGal) with pendant galactose and (*l*)-lysine groups/moieties were prepared via RAFT polymerization (Scheme 1). First, HEMA-Boc-Lys monomer was synthesized according to our previous work [39], the glycomonomer 6-O-methacryloyl-1,2,3,4-di-O-isopropylidene-galactopyranose (MAIGal) was prepared according to the literature [40]. The synthesis routes and characterization of the monomers were shown in supporting information (Scheme S1 and Figure S1). The homopolymer $PHMLBoc_{40}$ was obtained as a precursor via RAFT polymerization of HEMA-Boc-Lys monomer by using AIBN/4-cyanopentanoic acid dithiobenzoate system. Then MAIGal monomer was further polymerized by employing $PHMLBoc_{40}$ precursor as a Macro-chain-transfer-agent (MacroCTA) and two diblock glycopolymers containing different galactose ratios ($PHMLBoc_{40}$-*b*-$PMAIGal_3$ and $PHMLBoc_{40}$-*b*-$PMAIGal_{15}$) were obtained by adjusting the feeding ratio of MAIGal monomers and $PHMLBoc_{40}$ MacroCTA. For comparison, two statistical glycopolymers P($HMLBoc_{40}$-*st*-$MAIGal_4$) and P($HMLBoc_{40}$-*st*-$MAIGal_{13}$) were prepared through RAFT polymerization of MAIGal and HEMA-Boc-Lys monomers with predetermined feeding ratios. The structures of these polymers were characterized by ^{1}H NMR (Figure 1) and GPC (Figure 2). As shown in Figure 1, the average degree of polymerization of the MAlGal monomers $DP_{(MAIGal)}$ was calculated via the formula: $DP_{(MAIGal)} = (I_{a+b}-I_c)\times 80/I_d$. As shown in Figure 2, symmetric peaks were observed with comparatively low molecular weight distribution (M_w/M_n<1.35), indicating the synthesized glycopolymers possessed defined molecular structures, which might benefit for the elucidation of their chemical structure-biological property relationships.

Finally, cationic homopolymer PHML, block polymers $PHML_{40}$-*b*-$PMAGal_3$, $PHML_{40}$-*b*-$PMAGal_{15}$, and statistical polymers P(HML_{40}-*st*-$MAGal_4$), P(HML_{40}-*st*-$MAGal_{13}$) were obtained via TFA-mediated deprotection. The structures of the $PHML_{40}$-*b*-MAGal and P(HML_{40}-*st*-MAGal) cationic polymers were shown in Scheme 1 (The dithiobenzoate in the cationic polymers may be

decomposed after TFA-deprotection [41], so the dithiobenzoate end groups were removed and replaced with an asterisk *). Taking P(HML_{40}-*st*-$MAGal_{13}$) as an example, the ^1H NMR and FTIR characterization were shown in Figure S2 and Figure S3, respectively. It could be seen that the strong peaks at δ=1.36~1.42 ppm (acetal and Boc protecting groups) remarkably decreased (Figure S2), and the amide proton signal at 6.6 and 7.0 ppm disappeared along with the appearance of the new protonated amine signal at 8.1 and 8.8 ppm, which indicated the complete removal of the acetal and Boc protecting groups. In Figure S3, the stretch vibration signal of methyl group for the acetal and Boc protecting groups ($\nu_{C\text{-}CH3}$) at 1366 cm^{-1} disappeared along with the appearance of the hydroxyl group signal ($\nu_{O\text{-}H}$) at 3431 cm^{-1}, further confirming the structure of the P(HML_{40}-*st*-$MAGal_{13}$). The results demonstrated the successful preparation of the cationic glycopolymers.

3.2. pDNA binding affinity of the glycopolymers by agarose gel electrophoresis

pDNA binding affinities of the synthesized cationic diblock glycopolymers (PHML-*b*-PMAGal) and statistical glycopolymers (P(HML-*st*-MAGal)) were evaluated by agarose gel electrophoresis with the cationic homopolymer PHML as the control. As shown in Figure 3, all the cationic polymers were able to retard pDNA completely at the N/P charge ratio of 1, which might due to the strong pDNA binding affinity of the primary amino groups (pK_a=10.8) on the (*l*)-lysine moiety [42]. Noteworthy, different from some PEG-containing cationic polymers, introduction of galactose moieties into poly-(*l*)-lysine cationic polymers did not reduce the pDNA binding affinity, which might be partially attributed to the hydrogen bond-mediated interactions between the galactose moiety and pDNA [43]. Moreover, the results indicated that the PHML-*b*-PMAGal and P(HML-*st*-MAGal) cationic glycopolymers possessed high pDNA binding affinity, which made them ~~as~~ efficient cargoes for pDNA loading.

3.3. Average particle size and zeta potential measurements

Average particle size and zeta potential of polymers/pDNA polyplexes were essential factors for cytotoxicity, cellular uptake and gene transfection efficiency [34]. Herein, the average particle sizes of the cationic glycopolymers/pDNA polyplexes at various N/P charge ratios were measured by DLS with the homopolymer PHML as a control. As shown in Figure 4, all the polyplexes displayed average size range of 100~300 nm within the N/P charge ratio of 10~100. It could be found that the

$PHML_{40}$-*b*-$PMAGal_{15}$/pDNA and P(HML_{40}-*st*-$MAGal_{13}$)/pDNA (N/P=40) polyplexes, which containing higher percentage of galactose moieties (16.2% and 14.3%, respectively), showed comparatively larger particle size than the other polyplexes, that might due to the formation of a galactose-containing hydrophilic shell/corona on the surface of polyplex payloads by the strong hydration effect of galactose moieties. Moreover, morphology of the $PHML_{40}$/pDNA, $PHML_{40}$-*b*-$MAGal_3$/pDNA and P (HML_{40}-*st*-$MAGal_4$)/pDNA polyplexes was examined by transmission electron microscopy (TEM). As shown in Figure S4, all of the polyplexes formed spherical-shaped nanoparticles with the size range of 30~110 nm, which was smaller than the size measured by DLS, due to the shrinkage of the nanoparticles under drying process during the preparation of TEM samples [35, 44]. Besides, the zeta potentials of the polyplexes were measured by DLS. As shown in Figure 4b, the polyplexes displayed positive surface potentials (+30.2~+46.3 mV) at N/P charge ratios from 10 to 100, for each polyplexes, the zeta potential almost maintained at the same level and showed less dependence of the N/P charge ratios (N/P 10~100), suggesting the complete pDNA binding of the cationic polymers within the N/P range, due to the strong electrostatic interactions between the cationic lysine groups/moieties with pDNA, which is in accordance with the above electrophoresis results and our previous work [39]. Moreover, the relatively small particle size and positive surface potential of the polyplexes may benefit their cell surface adhesion and following intracellular uptake process [36], which may further improve the intracellular gene transfection capability.

3.4. Cytotoxicity

Cytotoxicity is one of the most important parameters for evaluating the safety of the non-viral gene vectors toward therapeutic application. Recently, it has been revealed that introducing of some natural moieties such as cholesterol, sugar and amino acids could improve biocompatibility and decrease cytotoxicity of polymeric gene vectors [34]. Herein, the cytotoxicity of cationic polymers PHML, PHML-*b*-PMAGal and P(HML-*st*-MAGal) were measured by MTT assay with the commercially available bPEI-25K as a control. As shown in Figure 5, severe cytotoxicity (relative cell viability, RCV<30%) was observed in H1299 cells when incubated with bPEI-25k at the dose up to 60 μg/mL, whereas PHML, $PHML_{40}$-*b*-$PMAGal_3$ and P(HML_{40}-*st*-$MAGal_4$) showed lower cytotoxicity (RCV>60%) than bPEI-25k at the same dose range. Noteworthy, the galactose-rich

cationic polymers $PHML_{40}$-*b*-$PMAGal_{15}$ and $P(HML_{40}$-*st*-$MAGal_{13})$ exhibited much lower cytotoxicity (RCV>80%) even at high concentration of 200 μg/mL, which indicated that introducing of biocompatible galactose moieties could decrease the cytotoxicity of cationic polymers. Similarly, previous literatures had reported sugar (cyclodextrin)-conjugation on some cationic dendrimer gene carriers could lower their cytotoxicity [45]. Moreover, the MTT results suggested that the cationic glycopolymers might be employed as comparatively safe vectors for gene delivery application.

3.5. *In vitro* luciferase gene transfection

In vitro gene transfection activity of PHML, PHML-*b*-PMAGals and P(HML-*st*-MAGal)s cationic polymers were evaluated under the presence of serum (10% FBS) in H1299 cells, with commercially available "gold standard" bPEI-25K as the control. As shown in Figure 6, homopolymer PHML showed its optimum transfection efficiency of 4.5-fold higher than that of bPEI-25K, the low-galactose-content cationic glycopolymers $PHML_{40}$-*b*-$PMAGal_3$ and $P(HML_{40}$-*st*-$MAGal_4)$ showed their highest transfection efficiency at the N/P ratio of 40, 1.4~6.8-fold higher than the transfection level of the bPEI-25k (**P<0.05). However, the high-galactose-content cationic glypolymers $PHML_{40}$-*b*-$PMAGal_{15}$ and $P(HML_{40}$-*st*-$MAGal_{13}$ showed comparatively lower transfection efficiencies than their low-galactose-content counterparts. The lower gene transfection efficiency of the high-galactose-content cationic polymers might due to the surface charge shielding effect of their excess galactose moieties, which hindered the effective adhesion of the cationic lysine moieties with negatively-charged cell membrane, thus further decreased the cellular uptake capability and subsequent gene expression. Noteworthy, the statistical glycopolymer $P(HML_{40}$-*st*-$MAGal_4)$ showed higher transfection capability than the block glycopolymer $PHML_{40}$-*b*-$PMAGal_3$, which have similar chemical component but different copolymer sequence/ arrangement, indicating that the gene transfection efficiency depends to some extent on the copolymer sequence/arrangement of the cationic glycopolymers. Similarly, Ahmed et al[29] observed similar transfection trend on a series of glucose-containing cationic glycopolymers, they supposed that the gene transfection difference might be attributed to the different interactions between the sequence-varied cationic glycopolymers and negatively-charged serum proteins.

To further evaluate the practical applications of the cationic glycopolymers in different cell lines under serum conditions (10% FBS), based on the transfection results in H1299 cells, the optimized

statistical cationic glycopolymer P(HML_{40}-*st*-$MAGal_4$) polyplexes (N/P=40) was utilized as the transfection model. As shown in Figure 7, the P(HML_{40}-*st*-$MAGal_4$) polyplexes showed obviously higher luciferase gene transfection efficiency (4.8~87-fold) than the "gold standard" bPEI-25K in SK-HEP-1, MCF-7, CHO, HeLa and COS-7 cells. The results suggested that the statistical cationic glycopolymer P(HML_{40}-*st*-$MAGal_4$) might be employed as a serum-compatible and high efficient transfection agent for cellular gene delivery and practical gene therapy.

3.6. Endocytosis mechanism/pathway of the P(HML_{40}-*st*-$MAGal_4$)/pDNA polyplexes

It had been revealed that gene/drug delivery efficiency of nano-delivery systems greatly relied on their endocytosis mechanism/pathway [46], to our knowledge, the study on endocytosis pathway of cationic glycopolymer vectors/pDNA complexes are still rare. Herein, in order to elucidate the endocytosis pathway of the P(HML_{40}-*st*-$MAGal_4$)/pDNA polyplexes (N/P=40, optimized condition) under serum environment (10% FBS), we investigated the luciferase expression in the presence of various endocytosis-specific inhibitors [47]. The H1299 cells transfected with P(HML_{40}-*st*-$MAGal_4$)/ pDNA polplexes (N/P=40) in the absence of the inhibitors was set as the control (luciferase expression: 100%). As shown in Figure 8, the luciferase expression of the P(HML_{40}-*st*-$MAGal_4$)/ pDNA polyplexes obviously decreased with the addition of M-β-CD (62.3 %) and nocodazole (18.2 %) respectively, indicating the P(HML_{40}-*st*-$MAGal_4$)/pDNA polplexes entered into H1299 cells mainly through the Caveolae-mediated (or lipid-raft-mediated) endocytosis and microtubule-dependent pathway. Interestingly, with addition of the clathrin-mediated endocytosis inhibitor chlorpromazine, the luciferase tranfection increased to around 150% (1.5-fold). Breackmans et al [48] also reported similar results, which might be attributed to the proton-buffering effect of chlorpromazine. The related mechanism in detail is still not very clear until now. Moreover, the luciferase expression of the H1299 cells incubated with the P(HML_{40}-*st*-$MAGal_4$)/pDNA polplexes decreased to 86.2% with addition of macropinocytosis inhibitor amiloride, which indicated that the macropinocytosis might not be served as the dominant endocytosis pathway. In previous works, we disclosed that a series of arginine-bearing polymers with high gene transfection efficiency undergoes caveolae (lipid-raft) mediated endocytosis pathway and followed by endosome localization [47]. Similarly, Helenius et al [49] revealed that caveosome-endoplasmic reticulum localization was followed by caveolae-mediated endocytosis of the cationic cargoes. Thus, we deduced that the

caveolae-mediated (or lipid-raft-mediated) endocytosis pathway may contribute to the high transfection efficiency of the P(HML_{40}-*st*-$MAGal_4$)/pDNA polyplexes.

3.7. Intracellular trafficking and localization of the P(HML_{40}-*st*-$MAGal_4$)/pDNA polyplexes

In order to further explore the transfection mechanism, the intracellular trafficking and localization of the P(HML_{40}-*st*-$MAGal_4$)/Cy3-pDNA polyplexes under the presence of serum (10% FBS) were investigated by fluorescence microscopy in H1299 cells, and the endosome/lysosome of H1299 cells was stained by lysotracker kit [50]. As shown in Figure 9 (merged image), after transfection for 2 h, it could be observed that the red fluorescence of P(HML_{40}-*st*-$MAGal_4$)/Cy3-pDNA polyplexes were overlapped with the green fluorescence of lysotracker and resulted in obvious yellow fluorescence emission, indicating the polyplexes were entrapped in endosome/lysosome. After 6h incubation, the yellow fluorescence almost disappeared and the red and green fluorescence dots clearly separated, which indicated successful and efficient "lysosome escape" effect. The results might be attributed to the proton buffering effects of cationic (*l*)-lysine moieties, which was regarded as one of the crucial factors to achieve efficient gene transfection. Moreover, some of the polyplexes could be found distributed inside the H1299 cell nuclei (Figure S5). Recently, it has been reported that internalized sugar-containing nanoparticles demonstrated "Trojan horse effect" and be able to colocalized within various subcellular organelles such as endosome/lysosome, endoplasmic reticulum, Golgi apparatus, and so on [51]. Based on this, we expected that the cationic glycopolymers with certain sugar-moieties may possess sugar-mediated intracellular trafficking/ localization effect, which may further provide new approaches for improving gene/drug delivery efficacy by directing gene/drug payloads go through the probably efficient "sugar-mediated pathways". In addition, further research on the correlation between sugar/carbohydrate moieties and intracellular localization/trafficking manners of the glycopolymer-based gene/drug delivery systems is currently under investigation in our lab.

4. Conclusions

In summary, a series of block/statistical cationic glycopolymers PHML-*b*-PMAGal and P(HML-*st*-MAGal) with pendant (*l*)-lysine and galactose moieties were prepared via RAFT polymerization and following Boc-deprotection. All the synthesized cationic glycopolymers showed high pDNA binding affinity at low N/P charge ratio of 1. The average hydrodynamic particle

diameter (150~300 nm) and positive zeta potential (+30~45 mV) of the cationic glycopolymers/pDNA polyplexes were found suitable for intracellular uptake. MTT assay showed that the cationic glycopolymers had significantly lower cytotoxicity than bPEI-25K, which depended on the block/statistical polymer architecture and galactose contents. Moreover, it could be noticed that the statistical copolymer P(HML_{40}-*st*-$MAGal_4$) with 4.8% galactose content showed the highest gene transfection efficiency among the synthesized cationic glycopolymers in the presence of 10% FBS, much higher than the "gold standard" bPEI-25K in various (H1299, SK-HEP-1, MCF-7, CHO, HeLa and COS-7) cell lines. Endocytosis pathway analysis indicated that the P(HML_{40}-*st*-$MAGal_4$)/pDNA polyplexes entered into H1299 cells mainly through the caveolae-mediated (or lipid-raft-mediated) endocytosis pathway and greatly depended on microtubule. Moreover, the P(HML_{40}-*st*-$MAGal_4$)/pDNA polyplexes showed related fast cellular uptake capability and obvious endosome/lysosome escaping effect. In conclusion, the current results suggested the synthesized cationic glycopolymers might be served as potential candidates for safe and efficient gene delivery in practical applications.

Acknowledgements: The authors are indebted to the financial supports partially from the National Science Foundation of China (21174160, 21002116 and 21372251). The authors are also grateful to Prof. Xiangyang Shi and Dr. Xueyan Cao of Donghua University for his kind assistances in FACS measurements. Dr. Ruilong Sheng appreciates the Chinese Academy of Sciences (CAS) for the CAS-Canada Young Visiting Scientist Scholarship and Youth Innovation Promotion Association (YIPA) for the sponsorship. We also thank the senior scientist Dr. Wilms Baille from Université de Montréal for his help on the presentations in the manuscript.

Reference

1. D. He and E. Wagner, *Macromol. Biosci.*, 2015, **15**, 600-612.
2. D. W. Pack, A. S. Hoffman, S. Pun and P. S. Stayton, *Nat. Rev. Drug Discov.*, 2005, **4**, 581-593.
3. M. A. Mintzer and E. E. Simanek, *Chem. Rev.*, 2009, **109**, 259-302.
4. G. Lin, H. Zhang and L. Huang, *Mol. Pharm.*, 2015, **12**, 314-321.
5. J. Dai, S. Zou, Y. Pei, D. Cheng, H. Ai and X. Shuai, *Biomaterials*, 2011, **32**, 1694-1705.
6. S. K. Tripathy, H. B. Black, E. Goldwasser and J. M. Leiden, *Nat. Med.*, 1996, **2**, 545-550.

7. S. Son and W. J. Kim, *Biomaterials*, 2010, **31**, 133-143.
8. A. Abe, A. Miyanohara and T. Friedmann, *Gene Therapy*, 1998, **5**, 708-711.
9. R. Tang, R. N. Palumbo, L. Nagarajan, E. Krogstad and C. Wang, *J. Control. Release.*, 2010, **142**, 229-237.
10. H. Petersen, T. Merdan, K. Kunath, D. Fischer and T. Kissel, *Bioconjug. Chem.*, 2002, **13**, 812-821.
11. K. Knop, R. Hoogenboom, D. Fischer and U. S. Schubert, *Angew. Chem. Int. Ed.*, 2010, **49**, 6288-6308.
12. F. Dai and W. Liu, *Biomaterials*, 2011, **32**, 628-638.
13. Y. T. Chim, J. K. Lam, Y. Ma, S. P. Armes, A. L. Lewis, C. J. Roberts, S. Stolnik, S. J. Tendler and M. C. Davies, *Langmuir*, 2005, **21**, 3591-3598.
14. A. E. Smith, A. Sizovs, G. Grandinetti, L. Xue and T. M. Reineke, *Biomacromolecules*, 2011, **12**, 3015-3022.
15. S. P. Strand, M. M. Issa, B. E. Christensen, K. M. Varum and P. Artursson, *Biomacromolecules*, 2008, **9**, 3268-3276.
16. Y. Liu and T. M. Reineke, *Biomacromolecules*, 2010, **11**, 316-325.
17. Y. Liu, L. Wenning, M. Lynch and T. M. Reineke, *J. Am. Chem. Soc.*, 2004, **126**, 7422-7423.
18. Y. Liu and T. M. Reineke, *Bioconjug. Chem.*, 2007, **18**, 19-30.
19. S. R. S. Ting, G. Chen and M. H. Stenzel, *Polym. Chem.*, 2010, **1**, 1392-1412.
20. B. Voit and D. Appelhans, *Macromol. Chem. Phys.*, 2010, **211**, 727-735.
21. T. Azzam, A. Raskin, A. Makovitzki, H. Brem, P. Vierling, M. Lineal and A. J. Domb, *Macromolecules*, 2002, **35**, 9947-9953.
22. S. R. Popielarski, S. Mishra and M. E. Davis, *Bioconjug. Chem.*, 2003, **14**, 672-678.
23. J. Chang, X. Xu, H. Li, Y. Jian, G. Wang, B. He and Z. Gu, *Adv. Funct. Mater.*, 2013, **23**, 2691-2699.
24. K. Nomura and R. R. Schrock, *Macromolecules*, 1996, **29**, 540-545.
25. J. Bernard, X. Hao, T. P. Davis, C. Barner-Kowollik and M. H. Stenzel, *Biomacromolecules*, 2006, **7**, 232-238.
26. M. Ahmed and R. Narain, *Biomaterials*, 2013, **34**, 4368-4376.
27. M. Ahmed and R. Narain, *Biomaterials*, 2012, **33**, 3990-4001.
28. M. Ahmed, M. Jawanda, K. Ishihara and R. Narain, *Biomaterials*, 2012, **33**, 7858-7870.
29. M. Ahmed and R. Narain, *Biomaterials*, 2011, **32**, 5279-5290.
30. D. Sprouse and T. M. Reineke, *Biomacromolecules*, 2014, **15**, 2616-2628.
31. Y. Wu, M. Wang, D. Sprouse, A. E. Smith and T. M. Reineke, *Biomacromolecules*, 2014, **15**, 1716-1726.

32. L. Xue, N. P. Ingle and T. M. Reineke, *Biomacromolecules*, 2013, **14**, 3903-3915.

33. V. P. Taori, H. Lu and T. M. Reineke, *Biomacromolecules*, 2011, **12**, 2055-2063.

34. R. Sheng, T. Luo, H. Li, J. Sun, Z. Wang and A. Cao, *Colloid. Surf. B.*, 2014, **116**, 32-40.

35. R. Sheng, T. Luo, Y. Zhu, H. Li, J. Sun, S. Chen, W. Sun and A. Cao, *Biomaterials*, 2011, **32**, 3507-3519.

36. X. Xu, H. Yuan, J. Chang, B. He and Z. Gu, *Angew. Chem. Int. Ed.*, 2012, **51**, 3130-3133.

37. W.-D. Jang, K. M. Kamruzzaman Selim, C.-H. Lee and I.-K. Kang, *Prog. Polym. Sci.*, 2009, **34**, 1-23.

38. G. Moad, Y. K. Chong, A. Postma, E. Rizzardo and S. H. Thang, *Polymer*, 2005, **46**, 8458-8468.

39. J. Sun, T. Luo, R. Sheng, H. Li, S. Chen, F. Hu and A. Cao, *Macromol. Biosci.*, 2013, **13**, 35-47.

40. F. Suriano, O. Coulembier, P. Degée and P. Dubois, *J. Polym. Sci. A: Polym. Chem.*, 2008, **46**, 3662-3672.

41. J. Lu, C. Fu, S. Wang, L. Tao, L. Yan, D. Haddleton, G. Chen, and Y. Wei, *Macromolecules*, 2014, **47**, 4676-4683.

42. A. M. Funhoff, C. F. van Nostrum, G. A. Koning, N. M. E. Schuurmans-Nieuwenbroek, D. J. A. Crommelin and W. E. Hennink, *Biomacromolecules*, 2004, **5**, 32-39.

43. Y. Miura, *Polym. J.*, 2012, **44**, 679-689.

44. R. Sheng, F. An, Z. Wang, M. Li and A. Cao, *Rsc Adv.*, 2015, **5**, 12338-12345.

45. H. Arima, K. Motoyama and T. Higashi, *Adv. Drug Deliv. Rev.*, 2013, **65**, 1204-1214.

46. S. Zhang, H. Gao and G. Bao, *ACS Nano.*, 2015, **9**, 8655-8671.

47. H. Li, T. Luo, R. Sheng, J. Sun, Z. Wang and A. Cao, *Biomaterials*, 2013, **34**, 7923-7938.

48. D. Vercauteren, R. E. Vandenbroucke, A. T. Jones, J. Rejman, J. Demeester, S. C. De Smedt, N. N. Sanders and K. Braeckmans, *Molecular Therapy*, 2010, **18**, 561-569.

49. L. Pelkmans, J. Kartenbeck and A. Helenius, *Nat. Cell. Biol.*, 2001, **3**, 473-483.

50. R. Sheng, T. Luo, H. Li, J. Sun, Z. Wang and A. Cao, *Bioorg. Med. Chem.*, 2013, **21**, 6366-6377.

51. D. Benito-Alifonso, S. Tremel, B. Hou, H. Lockyear, J. Mantell, D. J. Fermin, P. Verkade, M. Berry and M. C. Galan, *Angew. Chem. Int. Ed.*, 2014, **53**, 810-814.

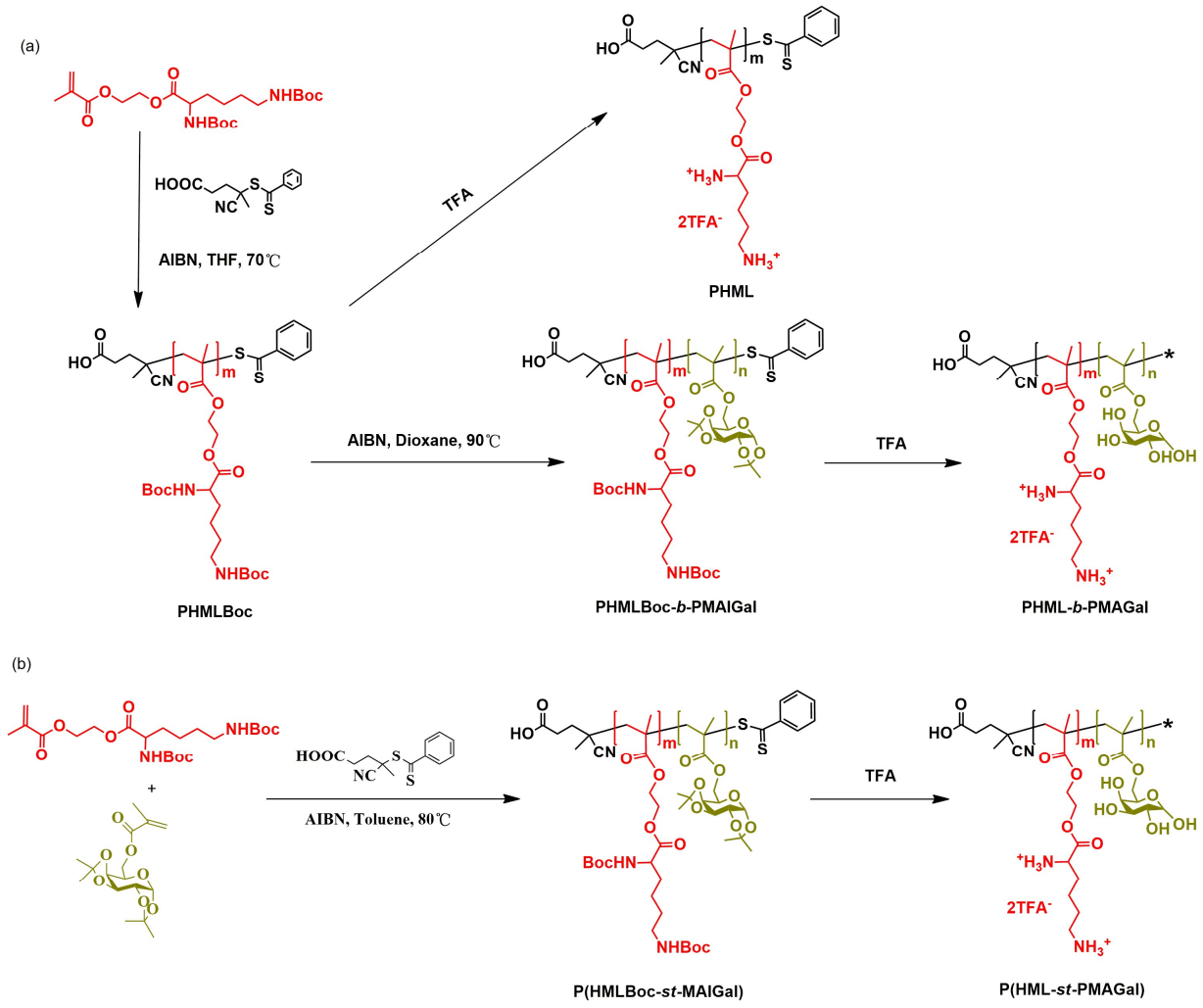

Scheme 1. Synthesis of the cationic homopolymer PHML, cationic block glycopolymers PHML-*b*-PMAGal and cationic statistical glycopolymers P(HML-*st*-MAGal) via RAFT polymerization and deprotection

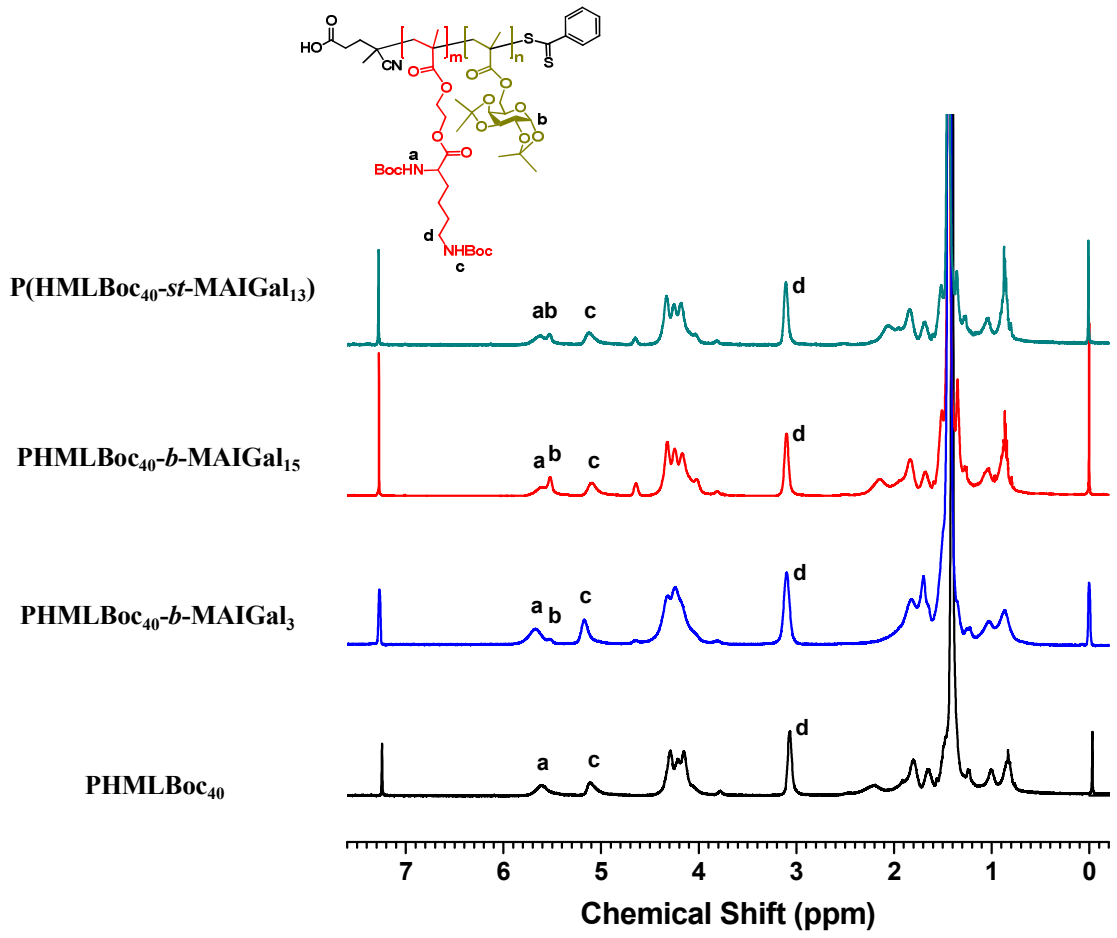

Figure 1. ^{1}H NMR spectra of the protected block/statistical glycopolymer precursors in $CDCl_3$.

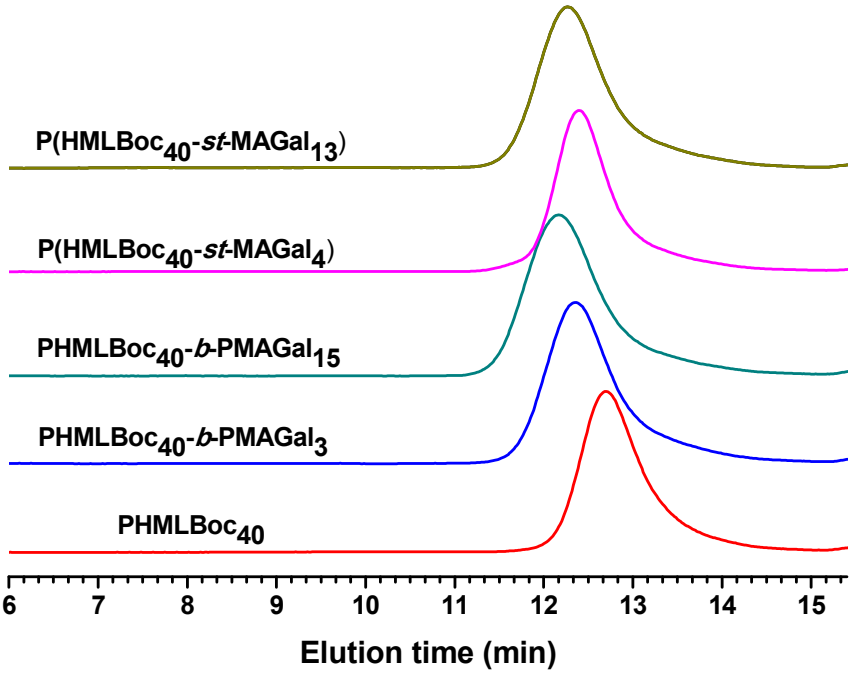

Figure 2. GPC elution traces for the PHMLBoc homopolymer, PHMLBoc-*b*-PMAIGal block copolymers and P(HMLBoc-*st*-MAIGal) statistical copolymers**.**

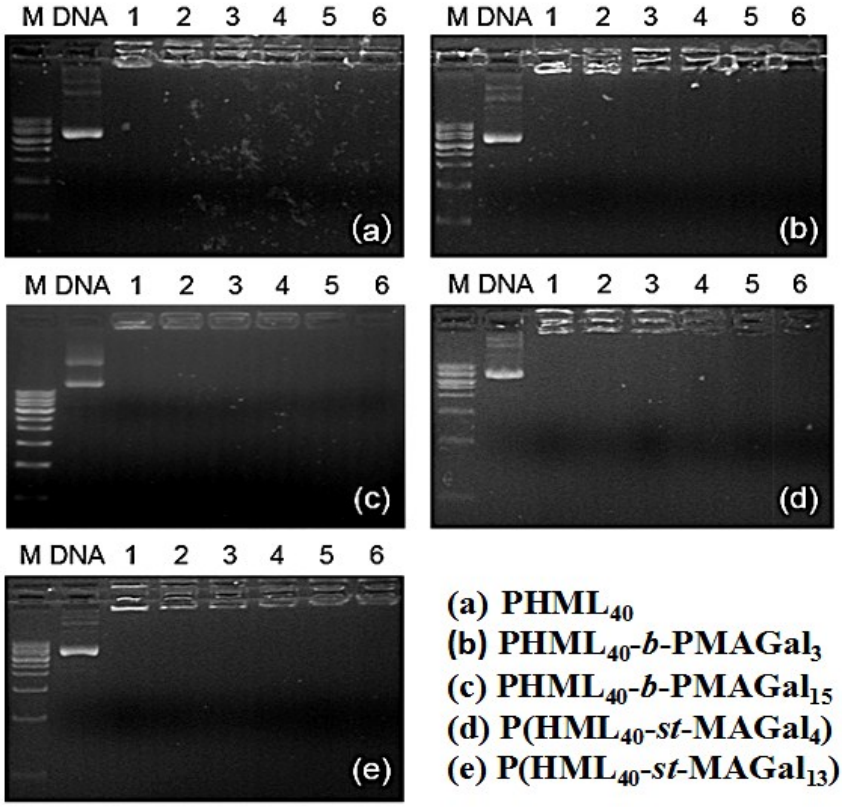

Figure 3. Agarose gel retardation assays of the cationic polymers/pDNA complexes at various N/P charge ratios. Lane 1: DNA marker; Lane 2: naked pDNA; Lanes 3~8: cationic polymers/pDNA polyplexes at the N/P ratios of 1~6, respectively

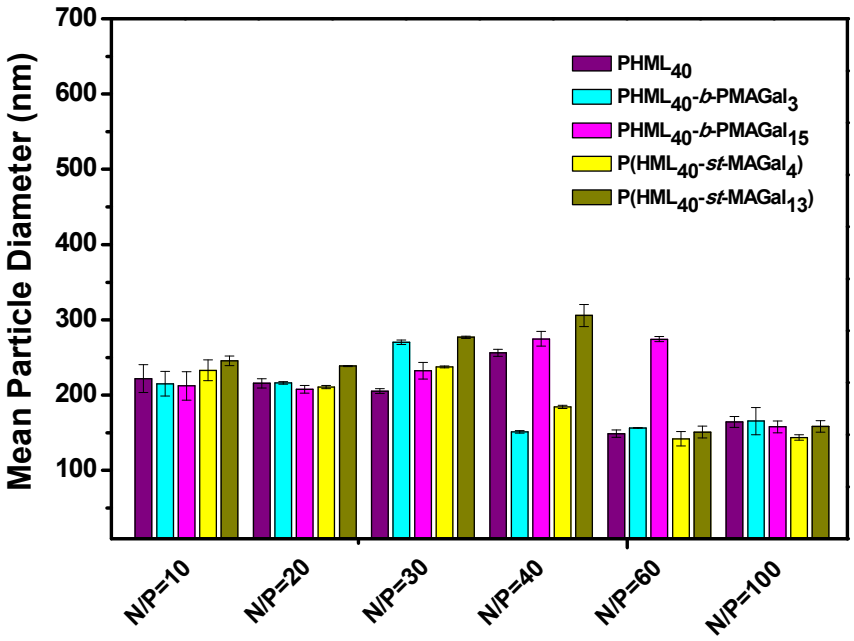

(a)

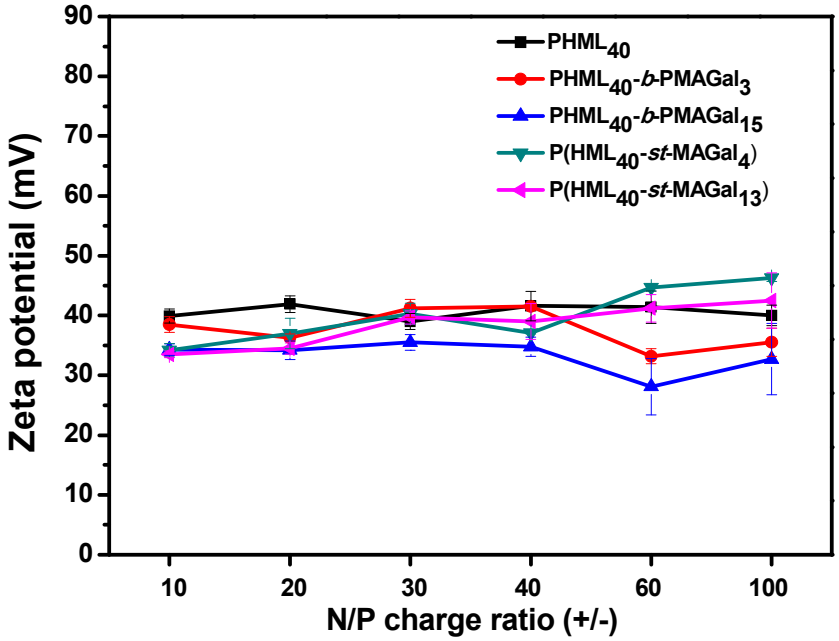

(b)

Figure 4. (a) Particle size and (b) zeta potential of the PHML, PHML-*b*-PMAGal and P(HML-*st*-MAGal)/pDNA polyplexes at various N/P ratios determined by DLS.

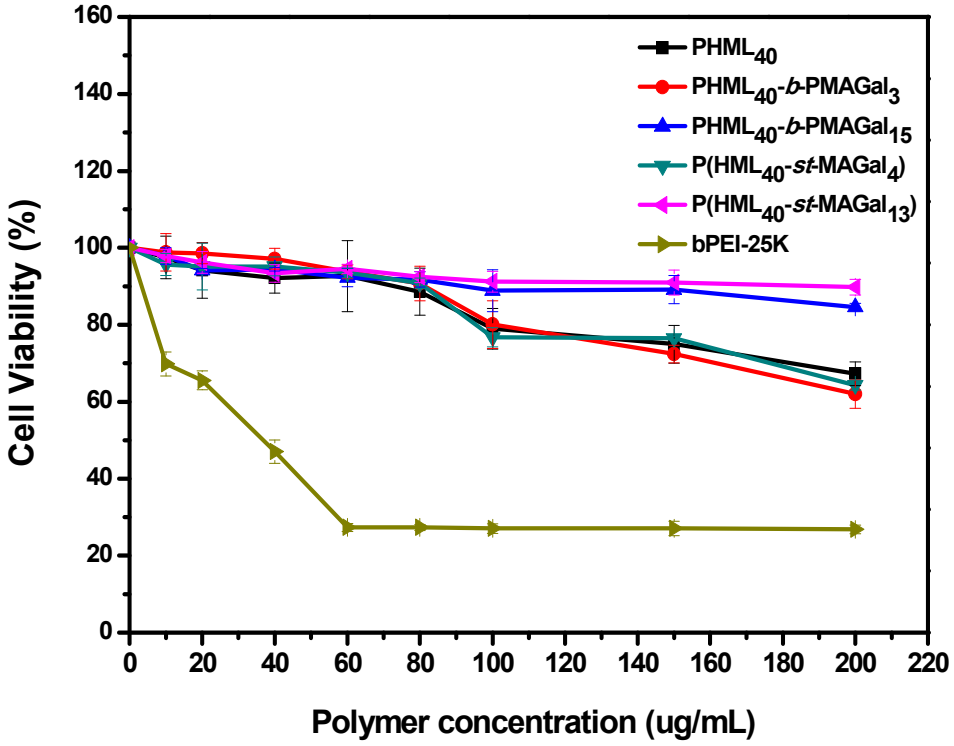

Figure 5. MTT cytotoxicity assay of the cationic polymers PHML, PHML-*b*-PMAGal and P(HML-*st*-MAGal) in H1299 cells under various dosages

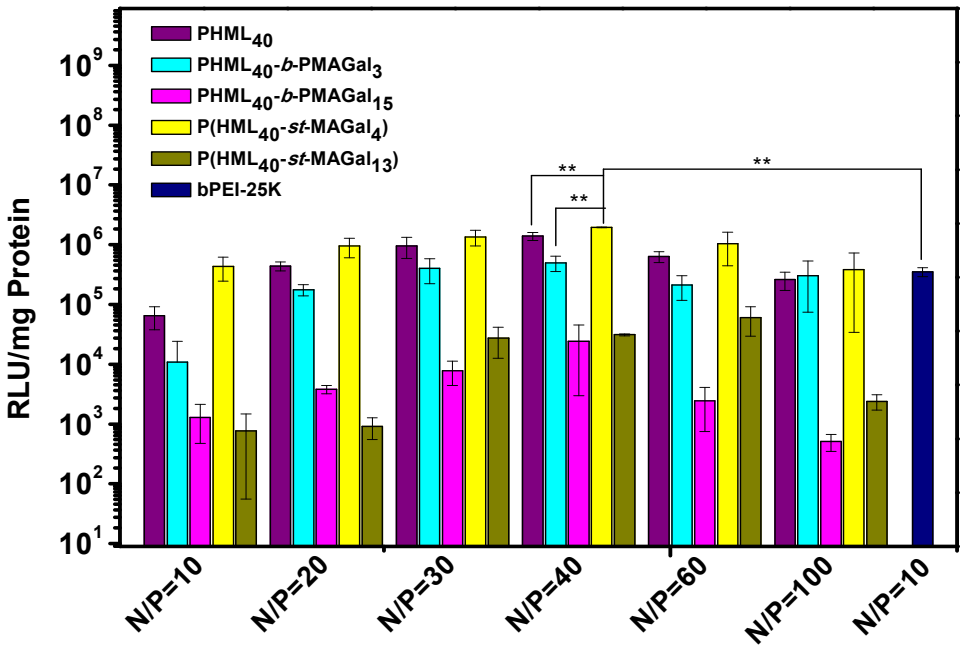

Figure 6. Luciferase gene transfection efficiency of the PHML, PHML-*b*-PMAGal and P(HML-*st*-MAGal) vectors under different N/P ratios with H1299 cells in the presence of 10% FBS (**P<0.05).

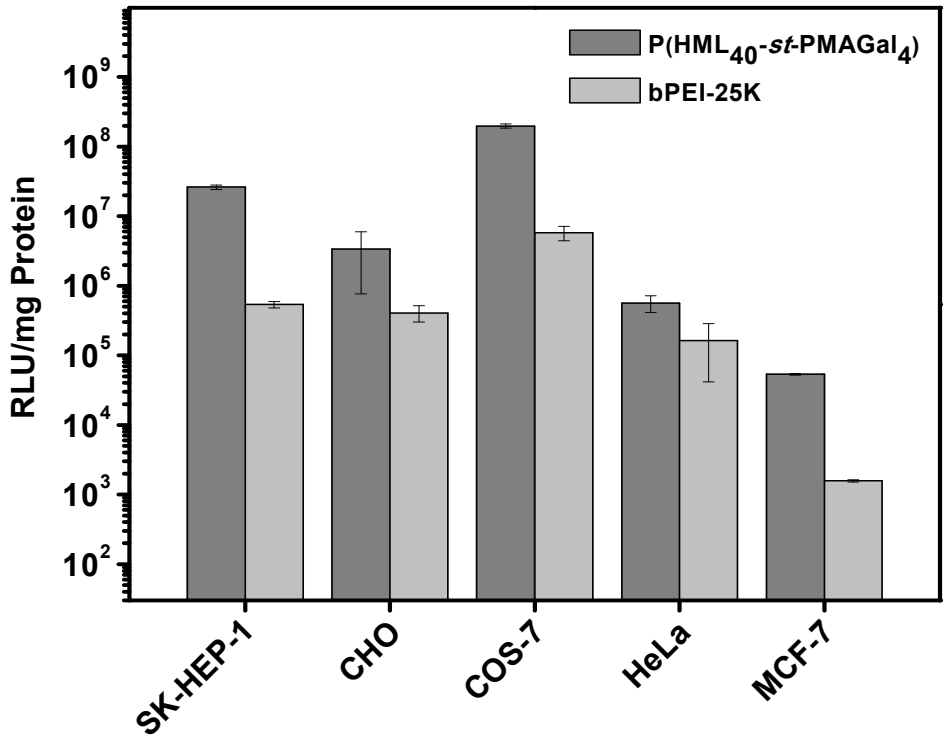

Figure 7. Luciferase gene transfection efficiency of the optimize glycopolymer P(HML_{40}-*st*-MAGal)/pDNA polyplexes determined in various cell lines in the presence of serum (10% FBS) at various N/P charge ratios. Transfection was performed at a dose of 1 μg pDNA/well (mean ±SD, n=3).

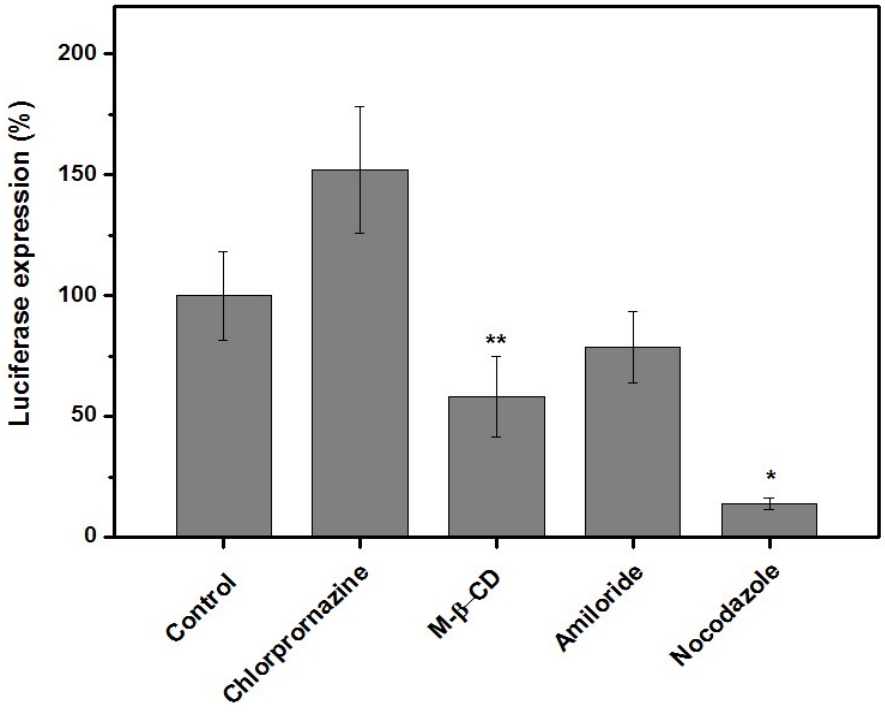

Figure 8. Luciferase gene transfection by the P(HML_{40}-*st*-$MAGal_4$) vector under N/P = 40 with H1299 cells in the RPMI 1640 medium containing 10% FBS in the presence of various endocytic inhibitors (*P<0.05, **P<0.01, ***P<0.001)**.**

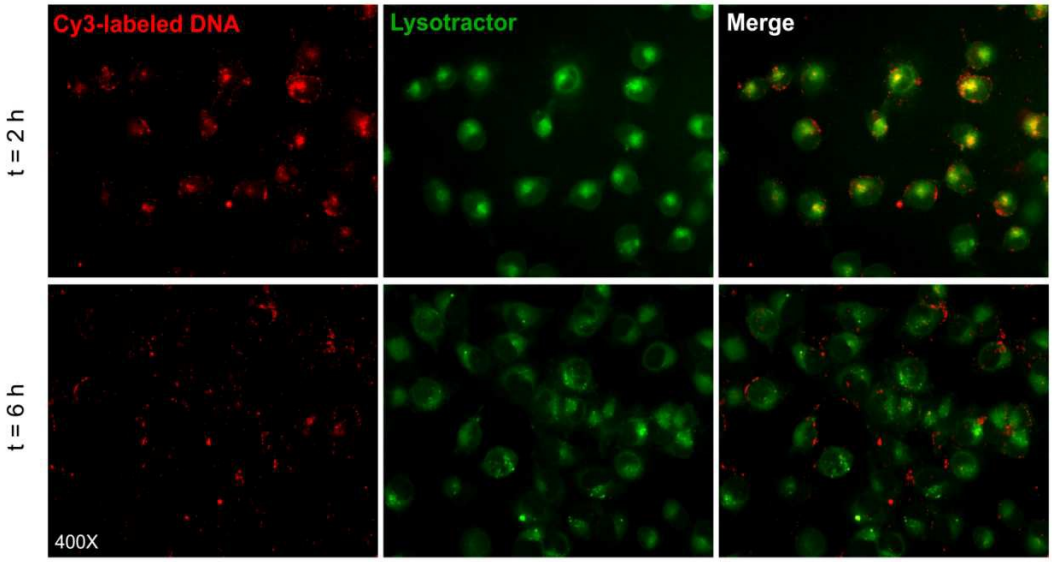

Figure 9. Fluorescence microscopic images (400×) of intracellular trafficking of the Cy3 labeling pDNA enveloped by P(HMLBoc$_{40}$-*st*-MAIGal$_4$) in H1299 cells recorded after 2 h, and 6 h of gene transfection (Green: lysotracker labeled lysosome, Red: Cy3 labeled pDNA).

Table 1. Synthetic results of the PHML homopolymer, PHML-*b*-PMAGal block copolymers and P(HML-*st*-MAGal) statistical copolymers.

Polymer Samples	$Mn_{,NMR}$/KDa[a]	$Mn_{,GPC}$/kDa[b]	Mw/Mn (PDI)	DP(HML)	DP(Gal)	MAGal cont[c]
Homopolymer						
$PHMLBoc_{40}$	18.6	21.1	1.19	40	0	0
Block copolymers						
$PHMLBoc_{40}$-*b*-$PMAIGal_3$	19.6	28.6	1.30	40	3	3.7%
$PHMLBoc_{40}$-*b*-$PMAIGal_{15}$	23.4	34.8	1.32	40	15	16.2%
Statistical copolymers						
P($HMLBoc_{40}$-*st*-$MAIGal_4$)	19.9	29.9	1.21	40	4	4.8%
P($HMLBoc_{40}$-*st*-$MAIGal_{13}$)	22.8	31.8	1.28	40	12	14.3%

Notes: [a]Molecular weights were estimated by ^{1}H NMR. [b]Data were obtained by GPC with THF as the eluent, and molecular weights and their distribution were calculated with polystyrene standards.[ca] Weight fraction of the MAGal moiety in the samples was calculated according to the MAIGal cont (%) = [DP(MAIGal)×248]/$M_{n,NMR}$, where 248 expresses molar mass of the MAGal moiety.

Graphical Abstract